JACS
JOURNAL OF THE AMERICAN CHEMICAL SOCIETY

Communication

pubs.acs.org/JACS

Charge Transport in Photoswitchable Dimethyldihydropyrene-Type Single-Molecule Junctions

Diego Roldan,[†,#] Veerabhadrarao Kaliginedi,[‡,#] Saioa Cobo,[†] Viliam Kolivoska,[‡] Christophe Bucher,[†,§] Wenjing Hong,[‡] Guy Royal,*[,†] and Thomas Wandlowski*[,‡]

[†]Département de Chimie Moléculaire, UMR CNRS-5250, Institut de Chimie Moléculaire de Grenoble, FR CNRS-2607, Université Joseph Fourier Grenoble I, BP 53, 38041 Grenoble Cedex 9, France

[‡]Department of Chemistry and Biochemistry, University of Bern, Freiestrasse 3, 3012 Bern, Switzerland

[§]Laboratoire de Chimie, UMR CNRS-5182, Ecole Normale Supérieure de Lyon, 46 allée d'Italie, 69364 Lyon, France

Supporting Information

ABSTRACT: The conductance properties of a photoswitchable dimethyldihydropyrene (DHP) derivative have been investigated for the first time in single-molecule junctions using the mechanically controllable break junction technique. We demonstrate that the reversible structure changes induced by isomerization of a single bispyridine-substituted DHP molecule are correlated with a large drop of the conductance value. We found a very high ON/OFF ratio (>10^4) and an excellent reversibility of conductance switching.

One current challenge in molecular electronics[1] is to build devices integrating molecules whose conductivity can be reversibly turned on and off by external stimuli such as light,[2] an electrochemical potential,[3] mechanical motion,[4] a magnetic field,[5] or temperature.[6] In this context, optically addressable molecules (photochromes) capable of undergoing structure and electronic changes upon irradiation appear as very attractive key components to build optoelectronic devices.[7]

Various experimental approaches have been employed to investigate charge transport properties of photochromic species in molecular ensembles as well as at the single-molecule level. The former include nanoparticle networks,[8] current-probe atomic force microscopy (CP-AFM),[9] scanning tunneling microscopy (STM),[10] liquid metal junctions,[11] and molecular layers sandwiched between lithographically prepared contact electrodes.[12] Experiments with a single or a few photochromic molecules have been addressed in matrix-isolation experiments,[13] mechanically controlled break junctions (MCBJ),[14] as well as in STM-BJ[15] and with two-terminal carbon nanotube devices.[16] The vast majority of experimental studies reported in the literature on this topic involve dithienylethene,[14c] stilbene,[15a] or azobenzene[11] as functional units. These examples demonstrated two challenges in constructing (single-molecule) light-driven switches: (i) reversibility and (ii) the significant attenuation of the ON/OFF ratio with the number of cycles.[7a,14d]

In this communication, we report the first single-molecule conductance measurements carried out with dimethyldihydropyrene (DHP)/cyclophanediene (CPD) isomers (Figure 1A).[17] DHP is a polycyclic π-conjugated unit, which can be optically converted into a less π-conjugated and colorless CPD isomer. This system is a rare example of a negative T-photochrome; i.e., the colorless open state (CPD) reversibly reverts both photochemically and thermally into the colored and more stable closed isomer (DHP). The polycyclic hydrocarbon skeleton of the DHP unit can furthermore be considered as a versatile molecular platform, which can be chemically functionalized in various ways. As a result, this molecular material is very attractive for the design of smart optoelectronic materials or molecular devices.

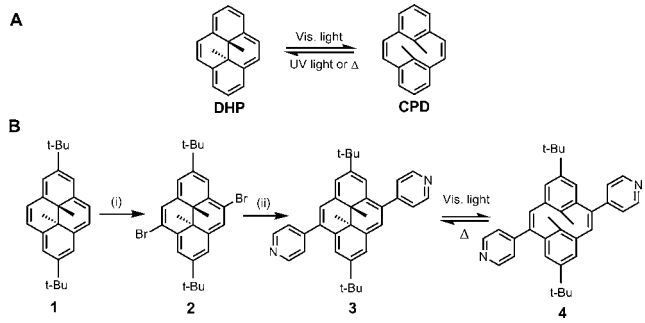

Figure 1. (A) DHP/CPD system. (B) Synthesis of **3**. Reagents and conditions: (i) NBS, DMF/CCl_4; (ii) 4-pyridinylboronic acid, $Pd(PPh_3)_4$, Na_2CO_3, THF/H_2O, reflux, 29%.

In this work, we have synthesized and investigated the conductance properties of **3** (Figure 1B), featuring two pyridine rings introduced on opposite sides of a DHP scaffold. Pyridine anchoring groups were selected to ensure efficient binding on the gold leads and to enable optimized electronic transport through the functional molecular wire.[18]

Preparation of **3** has been achieved in two steps starting from the 2,7-di-*tert*-butyldimethyldihydropyrene **1**.[17c,19] Bromination of the latter in the presence of *N*-bromosuccinimide led to the key intermediate **2**,[19b] which was then subjected to a palladium-catalyzed Suzuki cross-coupling reaction in the presence of 4-pyridinylboronic acid to afford **3** as a green solid with an overall 29% yield (Figure 1B).

The structure of **3** was confirmed by standard analytical methods (see Supporting Information (SI)). The singlet

Received: February 9, 2013
Published: April 11, 2013

   dx.doi.org/10.1021/ja401484j | J. Am. Chem. Soc. 2013, 135, 5974−5977

observed at −3.7 ppm in the ^{1}H NMR spectra of **3** recorded in deuterated chloroform is the most characteristic feature of the DHP skeleton. This signal is attributed to the resonance of the six equivalent internal methyl protons which are strongly shielded by the diatropic ring current induced by the delocalized electrons in the π-conjugated dihydropyrene unit. The absorption spectrum of **3** recorded in a chloroform/decane solution (1:4) exhibits two intense bands at 354 and 395 nm and two less intense bands in the 450−700 nm range (Figure 2).

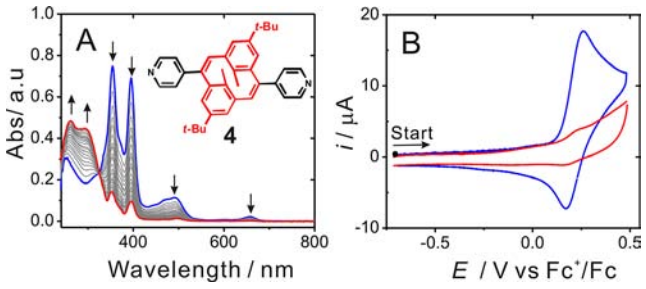

Figure 2. (A) Time-dependent evolution (with 10 min intervals) of the UV/vis spectra recorded during irradiation of a 2 × 10^{-5} M solution of **3** in $CHCl_3$/decane (1:4, v:v) with visible light at $\lambda \geq 490$ nm. (B) Cyclic voltammograms of **3** and **4** recorded in dichloromethane (0.1 M tetrabutylammonium perchlorate). The blue and red curves correspond to the closed **3** and the open **4** isomers, respectively.

The photoreactivity of **3** in solution was investigated through visible light irradiation experiments carried out at $\lambda \geq 490$ nm using a Xe−Hg lamp (500 W) equipped with a long-pass filter. All the experiments were carried out with a deoxygenated solution of **3**, prepared under an argon atmosphere. Under irradiation, the color of the solution changed progressively from green to colorless, which provides strong evidence for a chemical process accompanied with changes in photon absorption properties. The UV/vis spectra depicted in Figure 2 reveal a continuous decrease in the intensity of the main bands observed between 400 and 600 nm and the simultaneous appearance of new bands growing in the UV range. These changes can be unambiguously attributed to the photoconversion of **3** into its corresponding colorless open isomer **4** (Figure 2).[17b] This opening process is confirmed by ^{1}H NMR, as proved by a large shift from −3.7 to +1.5 ppm of the singlet signal of ^{1}H NMR corresponding to the internal methyl protons after irradiation at $\lambda \geq 490$ nm.

The reversibility of the photoisomerization process was then checked by irradiation of a solution of **4** at λ = 254 nm. The initial colorless sample turned progressively into green-brown. The UV/vis absorption spectra recorded simultaneously support the formation of the starting material **3**. However, this conversion is not quantitative, as revealed by the observation of additional signals attributed to species presumably produced through undesired side reactions stimulated by UV light (see SI for details). On the other hand, thermal activation was found to yield a quantitative back-isomerization of **4** to **3**, as unambiguously demonstrated in UV/vis and NMR experiments (see SI). The corresponding activation energy was estimated to be E_{act} = 147.8 kJ/mol on the basis of temperature-dependent spectroscopic measurements (see SI). These results demonstrate that the **3**/**4** couple can be reversibly converted back and forth through a combination of optical and thermal stimuli.

In addition, both isomers can be easily identified by electrochemical methods. The cyclic voltammogram (CV) of **3**, dissolved in CH_2Cl_2 containing tetra-n-butylammonium perchlorate (0.1 M), displays a reversible oxidation wave at $E_{1/2}$ = 0.21 V (versus the ferrocene/ferrocenium couple) corresponding to the transitory formation of $\mathbf{3}^{+\bullet}$ at the electrode interface, while under the same experimental conditions, the CV of **4** exhibits only a poorly defined redox process above 1.00 V (Figure 2B and SI).

The results of the solution-based photoisomerization studies motivated the design of a single-molecule conductance experiment. The conductance of junctions containing the closed form **3** (DHP) is expected to be much higher than that of junctions with the open form **4** (CPD) because of the significant difference in π-conjugation.[20] To demonstrate this, we employed a mechanically controllable break junction setup capable of operating in solution and two gold leads for trapping single molecules. Experimental aspects of the conductance measurements are summarized in the SI. For further details we refer to our previous publications.[21]

Figure 3A shows typical conductance−distance traces obtained in the presence of **3** (closed ON state, blue traces) and **4** (open OFF state, red traces) as recorded in decane/trichloromethane (4:1, v/v). Plateaus were observed in the conductance−distance traces in $1G_0 \leq G \leq 10G_0$, where $G_0 = 2e^2/h$ is the quantum conductance, which corresponds to the break of a monatomic Au−Au contact. Additional plateaus

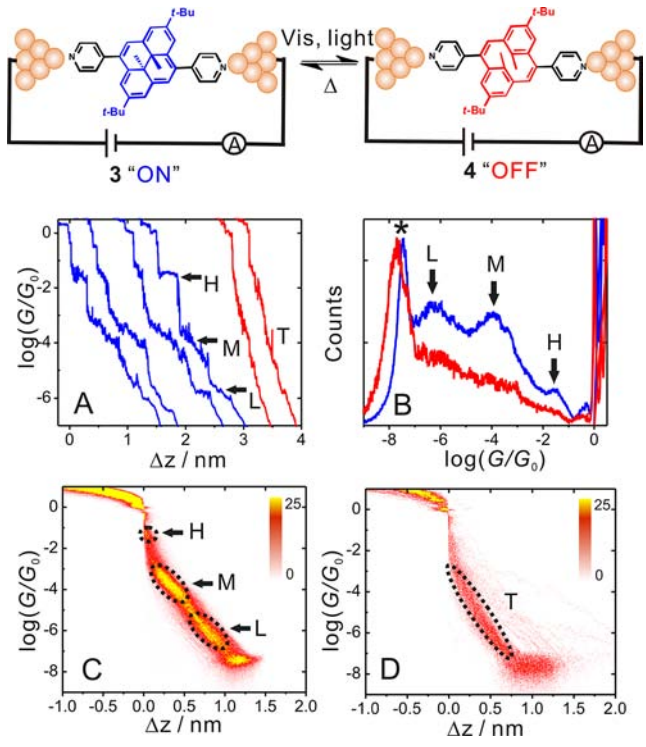

Figure 3. (A) Typical individual conductance versus relative displacement distance traces of **3** (ON state, blue) and **4** (OFF state, red) recorded in MCBJ experiments in $CHCl_3$/decane (1:4, v:v) containing 0.1 mM of the target molecules. (B) 1D logarithmic conductance histograms for the above systems constructed from 1000 individual curves and recorded with a bias voltage of 0.10 V. (C,D) 2D conductance histograms of **3** (C) and **4** (D).

dx.doi.org/10.1021/ja401484j | J. Am. Chem. Soc. 2013, 135, 5974−5977

evolving in $10^{-1}G_0 \geq G \geq 10^{-6.5}G_0$ in the experiments with **3** (blue traces) could be identified unambiguously as molecular junctions containing the closed-form isomer **3** (ON state). The noise limit of our MCBJ setup under the current experimental conditions is reached at $10^{-7.5}G_0$. Irradiation of a deoxygenated solution of **3** in the sealed liquid cell of the MCBJ stage with visible light (≥490 nm) for 30 min leads to the in situ generation of the open-form isomer **4** (OFF state). However, no plateaus were observed in the corresponding conductance−distance traces of molecular junctions with the photogenerated species **4**. The curves decay exponentially up to $10^{-7.5}G_0$.

Figure 3B displays the one-dimensional (1D) histogram on a logarithmic conductance scale as constructed from 1000 individual traces of **3** and **4** (ON and OFF states). The corresponding two-dimensional (2D) histograms of **3** and **4** are shown in Figure 3(C,D). The individual conductance−distance traces were normalized to the common point $\Delta z = 0$ at $G = 0.7G_0$, which is characterized by a sharp drop in conductance immediately after breaking the last Au−Au monatomic contact upon pulling the leads apart.[22] Quantitative analysis of the 1D and 2D histograms (Figures 3B−D) reveals the existence of three well-defined conductance features for **3**, whereas no features were observed in experiments with **4**. The conductance of single-molecule junctions containing the open-form isomer **4** is below our experimental detection limit. Control experiments with only the solvent (decane/trichloromethane) showed no conductance features, with or without irradiation by visible light (see SI for details). These experimental observations confirmed that the large conductance differences in single-molecule junctions of **3** and **4** could be attributed to the loss of aromaticity in **4**, revealing a distinctly different conjugation of both molecules[20] (see SI).

The presence of three distinct conductance features in the histograms of **3** [high (H), middle (M), and low (L)] could be attributed to the sequential formation of different configurations between the respective (single) molecule and the gold leads.[18,21b] Quantitative analysis of the 2D conductance (Figure 3C) and characteristic length (see SI) histograms leads to the following characteristic values: the high conductance state H is observed as conductance cloud in $10^{-2}G_0 \leq G \leq 10^{-1}G_0$, centered around the most probable value $G_H^* = 10^{-1.7}G_0$ at a relative lead displacement $\Delta z_H^* = 0.15$ nm. Considering the snapback distance $\Delta z_{corr} = 0.5 \pm 0.1$ nm upon breaking of the monatomic Au−Au contact,[18,21b,23] we estimate an absolute most probable gap distance $z_H^* = \Delta z_H^* + \Delta z_{corr} = 0.65 \pm 0.1$ nm. The middle conductance feature M dominates in $10^{-4.5}G_0 \leq G \leq 10^{-3.5}G_0$, with the most probable value $G_M^* = 10^{-4.0}G_0$ and the corresponding absolute gap distance $z_M^* = 1.28$ nm. The low conductance range L develops in $10^{-6.5}G_0 \leq G \leq 10^{-5.5}G_0$, with $G_L^* = 10^{-6.3}G_0$ and $z_L^* = 1.52$ nm. These data demonstrate that the single-molecule junction conductance of **3** decreases in distinct steps upon pulling the gold leads apart. Comparing the absolute displacement values z_i^* with the theoretical length of the closed isomer in an extended configuration of the molecular junction, $L_J^{Rel}(\mathbf{3}) = 1.55$ nm, and the typical length of a Au−N(pyridyl) bond $z_{Au\text{-}Py} = 0.21$ nm,[18] we tentatively rationalize the junction evolution as follows (see SI for details): immediately after breaking the Au−Au monatomic contact, the molecule slides along the tip of either of the two electrodes with its π-system attached to it (H), assumes a tilted orientation between the two electrodes (M), and finally transforms into a fully upright extended molecule (L) just before breaking. This scenario is supported by recent quantum-chemical and transport calculations in combination with MD-simulated stretching traces of pyridyl-terminated tolanes.[18] Details of the junction evolution and characteristic experimental and computed parameters are given in the SI.

To further elucidate the two-state conductance switching closed (**3**) ↔ open (**4**), we investigated sequential multiple in situ illumination and thermal return cycles at room temperature. All experiments were carried out using a deoxygenated solution of **3** under argon protection. The MCBJ measurements started with the closed form **3** (ON state). The three conductance features were clearly observed (see SI and Figure S5). We have chosen the mid-conductance range M with its most probable conductance value of $G_M^* = 10^{-4.0}G_0$ as reference. Next, we irradiated the solution in the MCBJ liquid cell for 30 min with visible light (≥490 nm), which led to the complete conversion of **3** (ON state) into **4** (OFF state).

The corresponding conductance histograms of **4** are displayed in Figure 3 and in the SI. Molecular junctions formed with **4** did not show any detectable conductance features within the accessible sensitivity range of our setup. Clearly, the single-molecule junction conductance of the OFF state is below $10^{-7.5}G_0$. Therefore, we have chosen this value as the upper limit of the conductance in the OFF state (Figure 4).

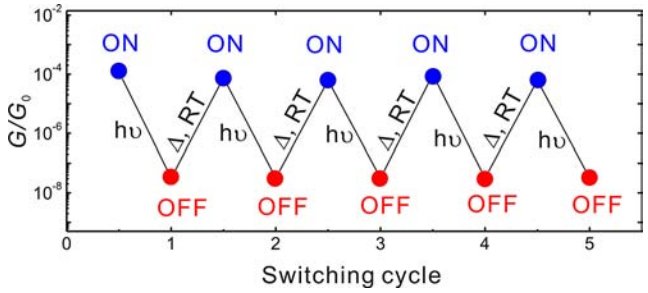

Figure 4. Five sequential, fully reversible cycles of the photothermally triggered in situ conductance switching between DHP (**3**) and CPD (**4**). The blue circles represent the most probable middle single junction conductance of the ON state **3**, and the red circles symbolize the upper limit of the OFF state **4**.

The ON state **3** recovers completely from the OFF state **4** upon thermal activation at room temperature during a waiting time of 45 min in the dark. The transformation of **4**↔**3** was monitored in the MCBJ setup as well as in UV/vis and NMR measurements under similar conditions. More than five of these combined photothermal switching cycles were monitored without detecting any attenuation in the corresponding conductance values of both states. Choosing the mid-conductance M state as reference, an ON/OFF ratio approaching 10^4 was estimated, i.e., 4 orders in magnitude. This ratio is significantly higher as compared to published data for other photochromic molecules, such as diarylethenes,[7a,12,14c,15b] azobenzenes,[7a] or redox switches,[3b,24] and demonstrates convincingly the unique properties of the DHP-type system studied in this communication.

To conclude, we have investigated the reversible photothermal switching of a bispyridine-appended dimethyldihydropyrene/cyclophanediene photochromic system employing UV/vis spectroscopy, NMR, and electrochemical measurements. Single-molecule conductance experiments using a mechanically controlled break junction setup in solution clearly revealed distinct changes in conductance between the fully conjugated ON state (**3**, closed form) and the broken conjugated OFF

dx.doi.org/10.1021/ja401484j | J. Am. Chem. Soc. 2013, 135, 5974−5977

state (**4**, open form). The photothermally triggered conductance switching between these two isomers is fully reversible, is stable over more than five sequential cycles, and reveals an excellent ON/OFF ratio approaching 10^4. This study demonstrates that DHP derivatives represent highly promising candidates for constructing addressable nanoscale molecular building blocks.

■ ASSOCIATED CONTENT

Supporting Information

Details on experimental procedures, and additional spectra and measurements. This material is available free of charge via the Internet at http://pubs.acs.org.

■ AUTHOR INFORMATION

Corresponding Author

thomas.wandlowski@dcb.unibe.ch; guy.royal@ujf-grenoble.fr

Author Contributions

[#]D.R. and V.K. contributed equally to this work.

Notes

The authors declare no competing financial interest.

■ ACKNOWLEDGMENTS

The authors gratefully acknowledge support through the PHC GERMAINE DE STAEL Program (2012-N° 26452ZG). This work was also supported by the Swiss National Science Foundation (200021-124643; NFP 62) and by the French Foundation for Nanosciences (Grenoble-POLYSUPRA Project) D.R. thanks the DCM (Grenoble) for financial support. The authors also thank Beatrice Gennaro (DCM, Grenoble) for assistance with NMR measurements.

■ REFERENCES

(1) Cuevas, J. C.; Scheer, E. *Molecular Electronics: An Introduction to Theory and Experiment*; World Scientific: Singapore, 2010.

(2) Irie, M. *Chem. Rev.* **2000**, *100*, 1685.

(3) (a) Simao, C.; Mas-Torrent, M.; Crivillers, N.; Lloveras, V.; Manuel Artes, J.; Gorostiza, P.; Veciana, J.; Rovira, C. *Nat. Chem.* **2011**, *3*, 359. (b) Darwish, N.; Diez-Perez, I.; Da Silva, P.; Tao, N.; Gooding, J. J.; Paddon-Row, M. N. *Angew. Chem., Int. Ed.* **2012**, *51*, 3203.

(4) Quek, S. Y.; Kamenetska, M.; Steigerwald, M. L.; Choi, H. J.; Louie, S. G.; Hybertsen, M. S.; Neaton, J. B.; Venkataraman, L. *Nat. Nanotechnol.* **2009**, *4*, 230.

(5) Jo, M.-H.; Grose, J. E.; Baheti, K.; Deshmukh, M. M.; Sokol, J. J.; Rumberger, E. M.; Hendrickson, D. N.; Long, J. R.; Park, H.; Ralph, D. C. *Nano Lett.* **2006**, *6*, 2014.

(6) Lu, Q.; Liu, K.; Zhang, H. M.; Du, Z. B.; Wang, X. H.; Wang, F. S. *ACS Nano* **2009**, *3*, 3861.

(7) (a) Feringa, B. L., Browne, W. R., Eds. *Molecular Switches*, 2nd ed.; Wiley-VCH: Weinheim, Germany, 2011. (b) van der Molen, S. J.; Liljeroth, P. *J. Phys.: Condens. Matter* **2010**, *22*, 133001.

(8) (a) Matsuda, K.; Yamaguchi, H.; Sakano, T.; Ikeda, M.; Tanifuji, N.; Irie, M. *J. Phys. Chem. C* **2008**, *112*, 17005. (b) van der Molen, S. J.; Liao, J.; Kudernac, T.; Agustsson, J. S.; Bernard, L.; Calame, M.; van Wees, B. J.; Feringa, B. L.; Schoenenberger, C. *Nano Lett.* **2009**, *9*, 76.

(9) (a) Mativetsky, J. M.; Pace, G.; Elbing, M.; Rampi, M. A.; Mayor, M.; Samori, P. *J. Am. Chem. Soc.* **2008**, *130*, 9192. (b) Uchida, K.; Yamanoi, Y.; Yonezawa, T.; Nishihara, H. *J. Am. Chem. Soc.* **2011**, *133*, 9239.

(10) Pace, G.; Ferri, V.; Grave, C.; Elbing, M.; von Haenisch, C.; Zharnikov, M.; Mayor, M.; Rampi, M. A.; Samori, P. *Proc. Natl. Acad. Sci. U.S.A.* **2007**, *104*, 9937.

(11) Ferri, V.; Elbing, M.; Pace, G.; Dickey, M. D.; Zharnikov, M.; Samori, P.; Mayor, M.; Rampi, M. A. *Angew. Chem., Int. Ed.* **2008**, *47*, 3407.

(12) Kronemeijer, A. J.; Akkerman, H. B.; Kudernac, T.; van Wees, B. J.; Feringa, B. L.; Blom, P. W. M.; de Boer, B. *Adv. Mater.* **2008**, *20*, 1467.

(13) (a) Kumar, A. S.; Ye, T.; Takami, T.; Yu, B.-C.; Flatt, A. K.; Tour, J. M.; Weiss, P. S. *Nano Lett.* **2008**, *8*, 1644. (b) Katsonis, N.; Kudernac, T.; Walko, M.; van der Molen, S. J.; van Wees, B. J.; Feringa, B. L. *Adv. Mater.* **2006**, *18*, 1397.

(14) (a) Kim, Y.; Garcia-Lekue, A.; Sysoiev, D.; Frederiksen, T.; Groth, U.; Scheer, E. *Phys. Rev. Lett.* **2012**, *109*, 226801. (b) Briechle, B. M.; Kim, Y.; Ehrenreich, P.; Erbe, A.; Sysoiev, D.; Huhn, T.; Groth, U.; Scheer, E. *Beilstein J. Nanotechnol.* **2012**, *3*, 798. (c) Kim, Y.; Hellmuth, T. J.; Sysoiev, D.; Pauly, F.; Pietsch, T.; Wolf, J.; Erbe, A.; Huhn, T.; Groth, U.; Steiner, U. E.; Scheer, E. *Nano Lett.* **2012**, *12*, 3736. (d) Dulic, D.; van der Molen, S. J.; Kudernac, T.; Jonkman, H. T.; de Jong, J. J. D.; Bowden, T. N.; van Esch, J.; Feringa, B. L.; van Wees, B. J. *Phys. Rev. Lett.* **2003**, *91*, 207402.

(15) (a) Martin, S.; Haiss, W.; Higgins, S. J.; Nichols, R. J. *Nano Lett.* **2010**, *10*, 2019. (b) Tam, E. S.; Parks, J. J.; Shum, W. W.; Zhong, Y.-W.; Santiago-Berrios, M. E. B.; Zheng, X.; Yang, W.; Chan, G. K. L.; Abruna, H. D.; Ralph, D. C. *ACS Nano* **2011**, *5*, 5115. (c) He, J.; Chen, F.; Liddell, P. A.; Andreasson, J.; Straight, S. D.; Gust, D.; Moore, T. A.; Moore, A. L.; Li, J.; Sankey, O. F.; Lindsay, S. M. *Nanotechnology* **2005**, *16*, 695.

(16) (a) Del Valle, M.; Gutirrez, R.; Tejedor, C.; Cuniberti, G. *Nat. Nanotechnol.* **2007**, *2*, 176. (b) Whalley, A. C.; Steigerwald, M. L.; Guo, X.; Nuckolls, C. *J. Am. Chem. Soc.* **2007**, *129*, 12590.

(17) (a) Muratsugu, S.; Kume, S.; Nishihara, H. *J. Am. Chem. Soc.* **2008**, *130*, 7204. (b) Mitchell, R. H. *Eur. J. Org. Chem.* **1999**, 2695. (c) Vila, N.; Royal, G.; Loiseau, F.; Deronzier, A. *Inorg. Chem.* **2011**, *50*, 10581.

(18) Hong, W.; Manrique, D. Z.; Moreno-Garcia, P.; Gulcur, M.; Mishchenko, A.; Lambert, C. J.; Bryce, M. R.; Wandlowski, T. *J. Am. Chem. Soc.* **2012**, *134*, 2292.

(19) (a) Tashiro, M.; Yamato, T. *J. Am. Chem. Soc.* **1982**, *104*, 3701. (b) Mitchell, R. H.; Ward, T. R.; Chen, Y. S.; Wang, Y.; Weerawarna, S. A.; Dibble, P. W.; Marsella, M. J.; Almutairi, A.; Wang, Z. Q. *J. Am. Chem. Soc.* **2003**, *125*, 2974.

(20) Markussen, T.; Stadler, R.; Thygesen, K. S. *Nano Lett.* **2010**, *10*, 4260.

(21) (a) Hong, W.; Valkenier, H.; Meszaros, G.; Manrique, D. Z.; Mishchenko, A.; Putz, A.; Garcia, P. M.; Lambert, C. J.; Hummelen, J. C.; Wandlowski, T. *Beilstein J. Nanotechnol.* **2011**, *2*, 699. (b) Kaliginedi, V.; Moreno-Garcia, P.; Valkenier, H.; Hong, W.; Garcia-Suarez, V. M.; Buiter, P.; Otten, J. L. H.; Hummelen, J. C.; Lambert, C. J.; Wandlowski, T. *J. Am. Chem. Soc.* **2012**, *134*, 5262.

(22) Mishchenko, A.; Zotti, L. A.; Vonlanthen, D.; Burkle, M.; Pauly, F.; Cuevas, J. C.; Mayor, M.; Wandlowski, T. *J. Am. Chem. Soc.* **2011**, *133*, 184.

(23) (a) Agrait, N.; Yeyati, A. L.; van Ruitenbeek, J. M. *Phys. Rep.-Rev. Sec. Phys. Lett.* **2003**, *377*, 81. (b) Yanson, A. I.; Bollinger, G. R.; van den Brom, H. E.; Agrait, N.; van Ruitenbeek, J. M. *Nature* **1998**, *395*, 783.

(24) Li, C.; Mishchenko, A.; Pobelov, I.; Wandlowski, T. *Chimia* **2010**, *64*, 383.